Manuscript prepared for Hydrol. Earth Syst. Sci.
with version 2014/09/16 7.15 Copernicus papers of the LaTeX class copernicus.cls.
Date: 22 December 2015

Analytical Drawdown Solution for Steady State Pumping Tests in Two-dimensional Isotropic Heterogeneous Aquifers

Alraune Zech[1] and Sabine Attinger[1,2]

[1]Department of Computational Hydrosystems, UFZ Helmholtz Centre for Environmental Research, Leipzig, Germany
[2]Institute for Geosciences, Friedrich Schiller University, Jena, German

Correspondence to: Alraune Zech (alraune.zech@ufz.de)

Abstract.

A new method is presented which allows to interpret steady state pumping test in heterogeneous isotropic transmissivity fields. In contrast to mean uniform flow, the pumping test drawdowns in heterogeneous media cannot be described by a single effective or equivalent value of hydraulic transmissivity. A radially depending description of transmissivity is required, including the parameters of log-transmissivity: mean, variance and correlation length. Such a model is provided by the upscaling procedure Radial Coarse Graining, which describes the transition of near well to far field transmissivity effectively. Based on this approach, an analytical solution for a steady state pumping test drawdown is derived. The so-called effective well flow solution is derived for two cases: the ensemble mean of pumping tests and the drawdown at an individual heterogeneous transmissivity field. The analytical form of the solution allows to inversely estimate the parameters of aquifer heterogeneity. This is shown making use of virtual pumping tests, for both cases the ensemble mean drawdown and pumping tests at individual transmissivity fields. The effective well flow solution reproduces the drawdown for two-dimensional pumping tests in heterogeneous media in contrast to Thiem's solution for homogeneous media. Multiple pumping tests at an individual transmissivity fields, combined in a sampling strategy, are analyzed making use of the effective well flow solution to show that all statistical parameters of aquifer heterogeneity can be inferred under field conditions. Thus, the presented method is a promising tool to estimate parameters of aquifer heterogeneity, in particular variance and horizontal correlation length of log-transmissivity fields from steady state pumping test measurements.

1 Introduction

Pumping tests are a widely used tool to identify horizontal hydraulic conductivity, which is the parameter determining the groundwater flow velocity. Analytical solutions of the radial flow equation are used in practice to analyze measured drawdowns. In general, these solutions assume a constant homogeneous hydraulic conductivity like Thiem's solution for steady state (Thiem, 1906):

$$h_{\text{Thiem}}(r) = -\frac{Q_{\text{w}}}{2\pi D K_{\text{h}}} \ln \frac{r}{R} + h(R)\,. \tag{1}$$

Thiem's solution (1) gives the hydraulic head $h_{\text{Thiem}}(r)$ depending on the radial distance r from the well for homogeneous horizontal hydraulic conductivity K_{h}. It is valid in a confined aquifer of thickness D with fully penetrating well and a constant discharge Q_{w}, $h(R)$ is a known reference head at an arbitrary distance R from the well.

In large scale pumping tests the vertical extension of the aquifer is negligible compared to horizontal aquifer extend. Thus, flow is assumed to be horizontal and modelled as two-dimensional. Hydraulic conductivity is then replaced by transmissivity, which is defined as the product of conductivity and aquifer thickness $T = K_{\text{h}} D$. In the following, transmissivity will be used instead of horizontal hydraulic conductivity, since the focus of the work will be on two-dimensional well flow.

Most natural aquifers exhibit geological heterogeneity in the sedimentary composition, which evolved from the complex geomorphological processes through which they were formed. In particular, transmissivity shows a strong spatial variability. Values measured in the field vary over orders of magnitude (Gelhar, 1993). Geostatistical distributions are generally used to capture the effects of aquifer heterogeneities. Transmissivity $T(\boldsymbol{x})$ is modelled as log-normally distributed spatial random function: $\log T(\boldsymbol{x}) = Y(\boldsymbol{x})$ is normally distributed with a Gaussian probability density function $\text{pdf}_Y(x) = \frac{1}{2\pi\sigma^2} \exp\left(-\frac{(x-\mu)^2}{2\sigma^2}\right)$ in uni-variate form with μ and σ^2 being the mean and the variance of Y, respectively. The correlation structure of transmissivity in space is captured by a covariance model $\text{Cov}\left[T(\boldsymbol{x}+\boldsymbol{s}), T(\boldsymbol{x})\right] = \exp\left(2\mu + \sigma^2 + \text{CV}_Y(\boldsymbol{s})\right)$.

In the stochastic framework, the solution of the radial flow equation with a log-normal distributed transmissivity is also a random spatial function. Since the solution of the stochastic differential equation is out of scope, the focus of investigation was on homogeneous substitute values for describing well flow effectively. As a first approach, Thiem's solution (1) was applied to pumping tests in heterogeneous media. However, this requires a representative transmissivity value T for the whole range of the depression cone (Matheron, 1967), which does not exist. Effective or equivalent descriptions of transmissivity in pumping tests were investigated, e.g. by Desbarats (1992); Sánchez-Vila et al. (1999); Neuman et al. (2007); Dagan and Lessoff (2007); Schneider and Attinger (2008) and many more. For a detailed review see Sánchez-Vila et al. (2006).

In contrast to mean uniform flow, the pumping test drawdowns in heterogeneous media cannot be described by a single constant value of transmissivity (Matheron, 1967). Different transmissivities characterize the behavior near and far from the well: the representative value close to the well is

the harmonic mean of the log-normal transmissivity $T_{\mathrm{H}} = \exp\left(\mu - \frac{1}{2}\sigma^2\right) = T_{\mathrm{G}} \exp\left(-\frac{1}{2}\sigma^2\right)$. With increasing distance from the well, the drawdown behavior is characterized by the effective transmissivity for uniform flow, which is the geometric mean $T_{\mathrm{G}} = \exp(\mu)$ for flow in two dimensional isotropic porous media.

It seems obvious, that a representative description of transmissivity for well flow needs to be a radially depending function, which interpolates between the harmonic and the geometric mean. The equivalent transmissivity T_{eq} is a well established approach of a radially depending description, visualized in Fig. 1a. $T_{\mathrm{eq}}(r) = -\frac{Q_{\mathrm{w}}}{2\pi(h(r)-h(r_{\mathrm{w}}))} \ln \frac{r}{r_{\mathrm{w}}}$ was derived from Thiem's solution (1) (Matheron, 1967; Indelman et al., 1996; Dagan and Lessoff, 2007). In this sense, the equivalent transmissivity T_{eq} is defined as the value for a homogeneous medium, which reproduces locally the same total outflow as observed in the heterogeneous domain of radius r. T_{eq} is strongly impacted by the reference point r_{w} and the corresponding head $h(r_{\mathrm{w}})$, which is generally chosen to be the drawdown at the well $h(r_{\mathrm{w}})$. Therefore, the equivalent conductivity stays close to the harmonic mean T_{H}, which is representative for the drawdown behavior at the well (Fig. 1a). It takes more than 20 correlation length for T_{eq} to reach the far field representative value of T_{G}.

It is important to mention, that T_{eq} is not constructed to reproduce the drawdown which was used for calculating T_{eq}. Strictly speaking, replacing the heterogeneous transmissivity field with the equivalent transmissivity in a single forward model does not give the drawdown, with which T_{eq} was constructed as visualized in Fig. 1b. Instead $h_{\mathrm{eq}}(r)$ stays close to Thiem's solution with T_{H} as homogeneous substitute value.

Schneider and Attinger (2008) introduced a novel approach to describe well flow effectively. They derived a radial adapted transmissivity $T_{\mathrm{RCG}}(r)$ by applying the upscaling technique Coarse Graining to well flow. $T_{\mathrm{RCG}}(r)$ does not only depend on the radial distance r but also on the statistical parameters of aquifer heterogeneity T_{G}, σ^2 and ℓ. $T_{\mathrm{RCG}}(r)$ captures the transition from near well to far field representative transmissivities, based on the radial distance to the well and the parameters of aquifer heterogeneity, as visualized in Fig. 1a.

In this study, an analytical solution for the hydraulic head $h_{\mathrm{efw}}(r)$ is presented, which is based on the Radial Coarse Graining transmissivity $T_{\mathrm{RCG}}(r)$ as an extension to the work of Schneider and Attinger (2008). Similar work has been done by (Zech et al., 2012) for pumping test in three dimensional porous media. The effective well flow solution $h_{\mathrm{efw}}(r)$ describes the mean depression cone of a pumping test in two dimensional heterogeneous media effectively. It can be interpreted as an extension of Thiem's formula (1) to log-normal distributed heterogeneous media. It accounts for the statistical parameters T_{G}, σ^2 and ℓ and thus allows to inversely estimate them from measured drawdown data. In contrast to existing head solutions for well flow, $h_{\mathrm{efw}}(r)$ is not limited to low variances, but is applicable to highly heterogeneous media with variances $\sigma^2 \gg 1$.

In a similar approach Neuman et al. (2004) presented a graphical approach to estimate the statistical parameters of random transmissivity on the basis of steady state head data. The authors

constructed a mathematical description for the apparent transmissivity $T_{\mathrm{a}}(r)$ as function of the radial distance to the well r from theoretical findings of near and far field representative transmissivity and a cubic polynomial interpolation in between. From $T_{\mathrm{a}}(r)$ the authors constructed type curves for the hydraulic head, depending on the variance σ^2 and the correlation length ℓ. Neuman et al. (2004) further gave a multi-point strategy to analyze virtually measured drawdown data by type curve matching including parameter estimation.

The Radial Coarse Graining approach is similar to that of Neuman et al. (2004) in the idea of deriving a solution for the head drawdown for well flow depending on the statistics of the random transmissivity using an effective radial depending transmissivity. Major differences are: (i) the Radial Coarse Graining Transmissivity $T_{\mathrm{RCG}}(r)$ is not based on results of Monte Carlo simulations, but is derived from upscaling with physically motivated approximations; (ii) the functional form of $T_{\mathrm{RCG}}(r)$ is different from the expression for T_{a} of Neuman et al. (2004); (iii) the effective well flow solution $h_{\mathrm{efw}}(r)$ is derived analytically by solving the head equation; providing a closed form mathematical expression instead of type curves; (iv) inverse parameter estimation can be done by minimizing the difference between the measured drawdown data and $h_{\mathrm{efw}}(r)$ instead of type curves matching. The effective well flow method will be tested in a similar multi-point sampling strategy to analyze measured drawdown data of individual heterogeneous transmissivity fields as done by Neuman et al. (2004) as well as others (Copty and Findikakis, 2004; Firmani et al., 2006).

The work is organized the following: Sect. 2 is dedicated to the method of Radial Coarse Graining and the derivation of the effective well flow head solution. The concept of Radial Coarse Graining is explained in detail. Furthermore it is distinguished between the effective well flow solution for an ensemble mean and single realizations of heterogeneous transmissivity fields. Section 3 contains the application of the effective well flow solution to simulated pumping tests. It is shown, that $h_{\mathrm{efw}}(r)$ reproduces the drawdown in heterogeneous media and can be used to inversely estimate the statistical parameters of aquifer heterogeneity for both, ensemble mean and single realizations. In Sect. 4, a sampling strategy is presented to infer the parameters of aquifer heterogeneity of an individual transmissivity fields from multiple pumping tests at multiple locations making use of $h_{\mathrm{efw}}(r)$. Concluding remarks are given in Sect. 5.

2 Radial coarse graining transmissivity and effective well flow head

2.1 Steady state well flow with radially depending transmissivity

The drawdown of a steady state pumping test with a radially depending transmissivity $T(r)$ is given as the solution of the differential equation:

$$0 = T(r)\left(\frac{1}{r}\frac{\mathrm{d}h}{\mathrm{d}r} + \frac{\mathrm{d}^2h}{\mathrm{d}r^2}\right) + \frac{\mathrm{d}T(r)}{\mathrm{d}r}\frac{\mathrm{d}h}{\mathrm{d}r} = \left(\frac{1}{r} + \frac{\mathrm{d}\ln T(r)}{\mathrm{d}r}\right)\frac{\mathrm{d}h}{\mathrm{d}r} + \frac{\mathrm{d}^2h}{\mathrm{d}r^2}\,. \tag{2}$$

The equation can be solved in $\frac{\mathrm{d}h}{\mathrm{d}r}$ by separation of variables, resulting in $\frac{\mathrm{d}h}{\mathrm{d}r} = C_1 \frac{1}{rT(r)}$. The hydraulic head $h(r)$ is then given as the solution of the integral

$$h(r_2) - h(r_1) = C_1 \int_{r_1}^{r_2} \frac{1}{rT(r)} \,\mathrm{d}r. \tag{3}$$

The integration constant C_1 is determined by the boundary condition. Supposing a constant flux boundary condition at the well, gives $Q_\mathrm{w} = -2\pi r_\mathrm{w} T(r_\mathrm{w}) \frac{\mathrm{d}h}{\mathrm{d}r}(r_\mathrm{w}) = -2\pi r_\mathrm{w} T(r_\mathrm{w}) \frac{C_1}{r_\mathrm{w} T(r_\mathrm{w})}$ and thus, $C_1 = -\frac{Q_\mathrm{w}}{2\pi}$.

Equation (3) is the general solution of the radial flow equation (2) for radially depending transmissivity, independent of the functional form of $T(r)$.

When comparing Eq. (3) with the definition of the equivalent transmissivity, it becomes obvious that T_eq is not constructed to solve the equation. The combination of both formulas results in $\int_{r_1}^{r_2} \frac{1}{rT(r)} \,\mathrm{d}r = \frac{1}{T_\mathrm{eq}(r)} \ln \frac{r_1}{r_2}$, which is only fulfilled, when $T(r)$ is constant in r.

2.2 Concept of Radial Coarse Graining

A radial-depending transmissivity for log-normally distributed media with Gaussian correlation structure was derived by Schneider and Attinger (2008), denoted as $T_\mathrm{RCG}(r)$. It is based on the upscaling approach Radial Coarse Graining which follows the basic idea of a spatial filtering of the flow equation appropriate to the non-uniform flow character of a pumping test.

The approach was further developed for three-dimensional well flow by Zech et al. (2012) introducing an effective well flow solution for the hydraulic head. Similarly, the concept of Radial Coarse Graining for two-dimensional well flow will be expanded in the following. The process can be best explained within five major steps:

1. Coarse Graining for uniform flow
2. Transfer of Coarse Graining to radial flow conditions
3. Overcome non-locality of head equation for non-uniform flow
4. Effective Radial Coarse Graining transmissivity
5. Derivation of effective well flow head

The first three steps will be discussed shortly in the following. Step 4 and 5 will be explained in detail in Sec.2.3 and Sec. 2.4.

The Coarse Graining approach for uniform flow (step 1) was introduced by Attinger (2003), including derivation, mathematical proof and numerical simulations. The author started at a spatially variable transmissivity field $T(\boldsymbol{x})$ and derived a filtered version $T_\lambda^\mathrm{CG}(\boldsymbol{x})$, where fluctuation smaller than a cut-off length λ are filtered out. The resulting upscaled Coarse Graining transmissivity field

$T_\lambda^{\mathrm{CG}}(\boldsymbol{x})$ represents a log-normal distributed field with a smaller variance $\langle\sigma^2\rangle_\lambda$, but larger correlation length $\langle\ell\rangle_\lambda$. Attinger (2003) showed, that the statistical parameters relate to the parameter of the unfiltered field by $\langle\sigma^2\rangle_\lambda \equiv \sigma^2 \frac{\ell^2}{\ell^2+\lambda^2/4}$ and $\langle\ell\rangle_\lambda \equiv \left(\ell^2+\lambda^2/4\right)^{1/2}$.

The concept of Coarse Graining can similarly be applied to non-uniform flow (step 2). The critical point when transferring the results of Attinger (2003) to radial flow is the Fourier back-transformation of the filtered head equation after localization. For uniform flow, this can be done due to the reasonable assumption of constant head gradient. For non-uniform flow, this assumption is not valid and thus, localization is not possible straight ahead.

A heuristic approach is taken to overcome the limitation of non-locality for well flow (step 3). Conditions of a quasi-constant head gradient are constructed by adapting the size of the volume elements over which flow takes place. The head gradient in well flow is proportional to the reciprocal of the distance to the well: $\nabla h(r) = \frac{h(r)-h(r+\Delta r)}{\Delta r} \propto \frac{1}{r}$. The gradient is constant for volumes of size proportional to r. The step can be understood as a change from an equidistant Cartesian coordinate system to a polar coordinate system with cell sizes increasing with distance to the center, where the pumping well is located. Under this adaption, localization can be performed and so the following steps of the Coarse Graining procedure.

The changed coordinate system impacts on the scaling procedure and the parameter λ. For uniform flow, λ is constant. Adapted to well flow, the scaling parameter needs to be proportional to r, because the filter width increases with distance to the well, thus $\lambda/2 = \zeta r$. The result is an upscaled log-normal distributed field $T_r^{\mathrm{RCG}}(\boldsymbol{x})$ with an arithmetic mean $T_{\mathrm{A}}^{\mathrm{RCG}}(r)$ and a filtered fluctuation term. The step was presented by Schneider and Attinger (2008). It is not performed in a mathematically straight way, but problem adapted to well flow conditions.

2.3 Radial Coarse Graining Transmissivity

Spatial heterogeneity is still resolved in $T_r^{\mathrm{RCG}}(\boldsymbol{x})$, although reduced to the amount relevant to the pumping test. A further step of averaging is necessary to derive an effective description of the transmissivity for well flow conditions. Thereby, two different aspects are of interest: (i) an effective transmissivity for an ensemble and (ii) effective transmissivity for an individual field.

A result for an effective ensemble description is derived by averaging $T_r^{\mathrm{RCG}}(\boldsymbol{x})$ appropriate to well flow condition. The averaging rule is determined by the boundary condition at the well, which is the harmonic mean for two-dimensional well flow (Dagan, 1989). Thus, the effective mean transmissivity, noticed by $T_{\mathrm{RCG}}(r)$, is calculated via the theoretical description of the harmonic mean for log-normal distributed fields making use of the variance of the coarsened transmissivity $\langle\sigma^2\rangle_r = \frac{\sigma^2}{1+\zeta^2 r^2/\ell^2}$:

$$T_{\mathrm{RCG}}(r) = T_{\mathrm{G}} \exp\left(-\langle\sigma^2\rangle_r/2\right) = T_{\mathrm{G}} \exp\left(-\frac{1}{2}\frac{\sigma^2}{(1+\zeta^2 r^2/\ell^2)}\right) \ , \tag{4}$$

where r is the distance to the well, T_{G} is the geometric mean, σ^2 is the variance and ℓ is the correlation length of the log-transmissivity $T(\boldsymbol{x})$. ζ is a factor of proportionality, which was determined to be $\zeta = 1.6$, as discussed in detail by Zech et al. (2012).

$T_{\mathrm{RCG}}(r)$ can be interpreted as interpolating function between the representative transmissivity at the well $T_{\mathrm{H}} = T_{\mathrm{G}} \exp\left(-\frac{1}{2}\sigma^2\right)$ to the far field value T_{G} depending on r, controlled by the correlation length ℓ (Fig. 1a).

An effective description of well flow transmissivity for an individual field is derived from Eq (4). The behavior of individual fields is different especially at the well due to a lack of ergodicity there. The local transmissivity at the well T_{well} is not identical to the harmonic mean T_{H} as expected for the ensemble, but refers to the specific value of transmissivity at the well location. An adapted radial coarse graining transmissivity accounts for local effects by replacing the harmonic mean $T_{\mathrm{H}} = T_{\mathrm{G}} \exp\left(-\frac{1}{2}\sigma^2\right)$ by T_{well}. In Eq. (4) this refers to substituting the variance by $-\frac{1}{2}\sigma^2 = \ln T_{\mathrm{well}} - \ln T_{\mathrm{G}}$ and thus,

$$T_{\mathrm{RCG}}^{\mathrm{local}}(r) = T_{\mathrm{G}} \exp\left(\frac{\ln T_{\mathrm{well}} - \ln T_{\mathrm{G}}}{1+\zeta^2 r^2/\ell^2}\right) = T_{\mathrm{well}}^{\frac{1}{1+\zeta^2 r^2/\ell^2}} T_{\mathrm{G}}^{\frac{\zeta^2 r^2/\ell^2}{1+\zeta^2 r^2/\ell^2}} \quad . \tag{5}$$

$T_{\mathrm{RCG}}^{\mathrm{local}}(r)$ interpolates between the specific transmissivity at the well T_{well} and the far field value T_{G} depending on the radial distance r and the correlation length ℓ.

2.4 Effective well flow head

Explicit results for the hydraulic head drawdown in steady state pumping test with a radially depending transmissivity are achieved by solving the integral in Eq. (3) making use of $T_{\mathrm{RCG}}(r)$ (Eq. 4). The result is the effective well flow head $h_{\mathrm{efw}}(r)$ is given by

$$\begin{aligned} h_{\mathrm{efw}}(r) = &- \frac{Q_{\mathrm{w}}}{4\pi T_{\mathrm{G}}} \exp\left(\frac{\sigma^2}{2}\right) \left(\Gamma\left(\frac{\sigma^2}{2}\frac{-\zeta^2 r^2/\ell^2}{1+\zeta^2 r^2/\ell^2}\right) - \Gamma\left(\frac{\sigma^2}{2}\frac{-\zeta^2 R^2/\ell^2}{1+\zeta^2 R^2/\ell^2}\right)\right) \\ &+ \frac{Q_{\mathrm{w}}}{4\pi T_{\mathrm{G}}} \left(\Gamma\left(\frac{\sigma^2}{2}\frac{1}{1+\zeta^2 r^2/\ell^2}\right) - \Gamma\left(\frac{\sigma^2}{2}\frac{1}{1+\zeta^2 R^2/\ell^2}\right)\right) + h_R\,, \end{aligned} \tag{6}$$

where r is the radial distance from the well, Q_{w} is the pumping rate, T_{G} is the geometric mean, σ^2 is the log-transmissivity variance, and ℓ is the correlation length. Again, ζ is the factor of proportionality determined to be 1.6 and R is an arbitrary distance from the well, where the hydraulic head $h(R) = h_R$ is known. $\Gamma(x) = \int_{-\infty}^{x} \frac{\exp(z)}{z}\,\mathrm{d}z$ is the exponential integral function. Details on the derivation of $h_{\mathrm{efw}}(r)$ can be found in the Appendix.

An approximate solution $h_{\mathrm{efw}}^{\mathrm{approx}}(r)$ is derived from Eq. (6) by making use of an approximation of $\Gamma(x)$. Details are given in the Appendix.

$$\begin{aligned} h_{\mathrm{efw}}^{\mathrm{approx}}(r) = &- \frac{Q_{\mathrm{w}}}{2\pi T_{\mathrm{H}}} \ln\frac{r}{R} - \frac{Q_{\mathrm{w}}}{4\pi T_{\mathrm{G}}} \left(\mathrm{e}^{\frac{\sigma^2}{2}} - 1\right) \\ &\cdot \left(\ln\frac{1+\zeta^2 R^2/\ell^2}{1+\zeta^2 r^2/\ell^2} + \frac{\sigma^2}{2}\frac{1}{(1+\zeta^2 r^2/\ell^2)} - \frac{\sigma^2}{2}\frac{1}{(1+\zeta^2 R^2/\ell^2)}\right) + h_R\,, \end{aligned} \tag{7}$$

$h_{\text{efw}}(r)$ is constructed to describe the mean drawdown of a pumping test in two dimensional heterogeneous media effectively. The drawdown curve of $h_{\text{efw}}(r)$ for a specific choice of parameters (Ensemble A of Table 1) is given in Fig. 1b in comparison to the equivalent drawdown $h_{\text{eq}}(r)$, as the solution of the radial flow equation using the equivalent transmissivity T_{eq}, based on the same statistical parameters.

The effective well flow solution can be adapted to analyze individual pumping tests by using $T_{\text{RCG}}^{\text{local}}(r)$ (Eq. 5) instead of $T_{\text{RCG}}(r)$ (Eq. 4). The local effective well flow solution $h_{\text{efw}}^{\text{local}}(r)$ is than given by Eq. (6) with $\frac{\sigma^2}{2}$ substituted by $-\ln\frac{T_{\text{well}}}{T_{\text{G}}}$ and T_{H} substituted by T_{well}.

The local effective well flow solution $h_{\text{efw}}^{\text{local}}(r)$ can be used to analyze drawdowns of single pumping tests in heterogeneous media as encountered in practice. The solution is adapted to the lack of ergodicity at the well, by using transformed parameters T_{well}, T_{G} and ℓ. The geometric mean T_{G} and the correlation length ℓ for a single realization should also be interpreted as local values, not necessarily representing the mean values of the entire field, but those of the pumping well vicinity. Owing to the nature of the pumping test, the drawdown signal does not sample the heterogeneity in transmissivity in a symmetric way, but the shape of the drawdown is mainly determined by the local heterogeneity close to well.

2.5 Impact of parameters

The analytical form of $h_{\text{efw}}(r)$ allows to analyze the impact of the statistical parameters T_{G}, σ^2 and ℓ on the drawdown. The drawdown behavior for different choices of parameters can be seen in Fig. 2, which is discussed in detail later on.

Every parameter impacts on the drawdown in a different region. The geometric mean T_{G} as representative value for mean uniform flow determines the far field behavior. The variance σ^2 determines the drawdown at the well due to the dependence of the near-well asymptotic value $T_{\text{H}} = T_{\text{G}} \exp\left(-\frac{1}{2}\sigma^2\right)$. The larger the variance the larger are the differences between T_{G} and T_{H} and the steeper is the drawdown at the well. Whereas, the correlation length ℓ determines the transition from near to far field behavior. s The asymptotic behavior of $h_{\text{efw}}(r)$ can easily be analyzed using approximate functional description in Eq. (7): for distances close to the well, thus $r \ll \ell$, $h_{\text{efw}}(r)$ converges to Thiem's solution with T_{H} as homogeneous substitute value. All terms, except the first one in Eq. (7), tend to zero or become constant. Thus, they are negligible compared to logarithmic first term for very small r,

$$\begin{aligned} h_{\text{efw}}^{\text{approx}}(r \ll \ell) &\approx -\frac{Q_{\text{w}}}{2\pi T_{\text{H}}} \ln\frac{r}{R} - \frac{Q_{\text{w}}}{4\pi T_{\text{G}}} \left(\mathrm{e}^{\frac{\sigma^2}{2}} - 1\right) \cdot \left(\ln\left(1 + \zeta^2 R^2/\ell^2\right) + \frac{\sigma^2}{2}\right) + h_R \\ &\approx -\frac{Q_{\text{w}}}{2\pi T_{\text{H}}} \ln\frac{r}{R} + h_R. \end{aligned}$$

For large distances from the well, i.e. $r \gg \ell$, the solution converges to Thiem's solution with T_{G} as homogeneous substitute value. The third and fourth term in Eq. (7) tend to zero and cancel out. The

ones in the second term can be neglected, thus

$$h_{\text{efw}}^{\text{approx}}(r \gg \ell) \approx -\frac{Q_\text{w}}{2\pi T_\text{H}} \ln \frac{r}{R} - \left(\frac{Q_\text{w}}{4\pi T_\text{H}} - \frac{Q_\text{w}}{4\pi T_\text{G}} \right) \cdot \ln \left(\frac{\zeta^2 R^2/\ell^2}{\zeta^2 r^2/\ell^2} \right) + h_R \approx -\frac{Q_\text{w}}{2\pi T_\text{G}} \ln \frac{r}{R} + h_R.$$

The larger the correlation length ℓ the longer takes the transition of the drawdown from near well to far field behavior. The influence of ℓ on $h_{\text{efw}}(r)$ vanishes quickly with increasing distance to the well. The drawdown reaches the far field behavior after approximately two correlation lengths $h^{\text{efw}}(r > 2\ell) = h_{\text{Thiem}}(r > 2\ell)$ with T_G as homogeneous substitute value (Fig. 1b). These findings are in line with the results of Neuman et al. (2004).

3 Robust estimation of statistical parameters

3.1 Numerical pumping tests

Numerical pumping tests in heterogeneous porous media were generated as artificial measurements. They were used to test the capability of $h_{\text{efw}}(r)$ in reproducing the mean drawdown and in estimating the underlying parameters of heterogeneity. Pumping tests were simulated using the finite element software OpenGeoSys. The software was successfully tested against a wide range of benchmarks (Kolditz et al., 2012). Results of a steady state simulation with homogeneous transmissivity were in perfect agreement with Thiem's analytical solution Eq. (1).

The numerical grid was constructed as a square of 256×256 elements with a uniform grid cell size of $1\,\text{m}$ except for cells in the vicinity of the pumping well. The mesh was refined in the range of $4\,\text{m}$ around the well, which ensures a fine resolution of the steep head gradients at the well. The well in the center of the mesh was included as a hollow cylinder with radius $r_\text{w} = 0.01\,\text{m}$. The constant pumping rate of $Q_\text{w} = -10^{-4}\,\text{m}^3\,\text{s}^{-1}$ was distributed equally to all elements at the well. At the radial distance $R = 128\,\text{m}$ a constant head of $h(R) = 0\,\text{m}$ was applied giving a circular outer head boundary condition.

Log-normally distributed, Gaussian correlated transmissivity fields were generated using a statistical field generator based on the randomization method (Heße et al., 2014). Multiple ensembles with different statistical parameter values were generated, including high variances up to $\sigma^2 = 4$ (Table 1). Ensemble A with $T_\text{G} = 10^{-4}\,\text{m}^2\,\text{s}^{-1}$, $\sigma^2 = 1$ and $\ell = 10\,\text{m}$ served as reference ensemble for specific cases. Every ensemble consists of $N = 5000$ realizations, which was tested as sufficiently large to ensure ensemble convergence.

Pumping test simulations were post-processed by performing an angular and an ensemble average. For every realization i, the simulated drawdown $\langle h_i(r,\phi) \rangle$ at the radial and angular location (r, ϕ) in polar coordinates was averaged over the four axial directions: $\langle h_i(r) \rangle = \sum_{\phi_j} \langle h_i(r, \phi_j) \rangle$. The ensemble mean was the sum over the angular mean of all individual realizations: $\overline{\langle h(r) \rangle} = \sum_{i=1}^{N} \langle h_i(r) \rangle$.

Non-linear regression was used to find the best fitting values for the statistical parameters, denoted by $\hat{T}_\text{G}$, $\hat{\sigma}^2$, and $\hat{\ell}$. The best fitting estimates were determined by minimizing the mean square error

of the difference between the analytical solution $h_{\mathrm{efw}}(r)$ and the measured drawdown samples $h(r)$: $\min_{T_\mathrm{G},\sigma^2,\ell}\sum_r \left(h(r)-h_{\mathrm{efw}}(r)\right)^2$ making use of the Levenberg–Marquardt algorithm. The reliability of the estimated parameters was evaluated using $95\,\%$-confidence intervals.

The estimation procedure was applied to the head measurements at every meter distance starting at the well up to a distance of $80\,\mathrm{m}$. The range beyond $80\,\mathrm{m}$ was not taken into account to avoid boundary effects. The range of $80\,\mathrm{m}$ includes at least 4 correlation lengths for all tested ensembles, which is sufficient to ensure convergence to the far field behavior. The question of the applicability of $h_{\mathrm{efw}}(r)$ on limited head data is of quite complex nature. For a detailed discussion on that issue the reader is referred to Zech et al. (2015).

3.2 Ensemble pumping test interpretation

First, the simulated ensemble means were analyzed making use of the ensemble version of $T_{\mathrm{RCG}}(r)$ and $h_{\mathrm{efw}}(r)$ (Eqs. 4 and 6). Simulated ensemble means $\overline{\langle h(r)\rangle}$ for multiple choices of statistical parameters T_G, σ^2 and ℓ are visualized in Fig. 2 in combination with $h_{\mathrm{efw}}(r)$ for the best fitting parameter estimates $\hat{T}_\mathrm{G}$, $\hat{\sigma}^2$, and $\hat{\ell}$. Input parameters as well as inverse estimation results for all tested ensembles are listed in Table 1.

The best fitting estimates show, that all three parameters could be inferred from the ensemble mean with a high degree of accuracy. The deviation of the geometric mean from the input value is in general less than $10\,\%$, only for high variances the deviations are up to $30\,\%$. Variances deviate in a range of $20\,\%$ and estimated correlation lengths are accurate within $10\,\%$ of the initial input parameter.

The confidence intervals of the estimates $\hat{T}_\mathrm{G}$ and $\hat{\sigma}^2$ are very small, showing a high sensitivity of the effective well flow solution $h_{\mathrm{efw}}(r)$ towards geometric mean and variance. The confidence intervals of the correlation length are larger due to the dependence of the estimate of $\hat{\ell}$ on the estimates $\hat{T}_\mathrm{G}$ and $\hat{\sigma}^2$. This is due to the fact, that the correlation length determines the transition from $\hat{T}_{\mathrm{well}} = \hat{T}_\mathrm{G}\exp\left(-\frac{1}{2}\hat{\sigma}^2\right)$ to $\hat{T}_\mathrm{G}$, which results in larger uncertainties in the estimates of $\hat{\ell}$.

3.3 Individual pumping test interpretation

In the following, pumping test drawdowns of individual transmissivity fields are interpreted based on the adaption version $h^{\mathrm{local}}_{\mathrm{efw}}(r)$ as discussed in Sect. 2.4. The drawdowns along the four axial directions as well as the radial mean for two realizations from Ensemble A ($T_\mathrm{G} = 10^{-4}\,\mathrm{m^2\,s^{-1}}$, $\sigma^2 = 1$, $\ell = 10\,\mathrm{m}$) are visualized in Fig. 3a and b.

Both realizations from Fig. 3a and b differ significantly in the value of the local transmissivity at the well. The analysis of the transmissivity fields at the well gave sampled values of $< T^{(\mathrm{a})}_{\mathrm{well}} >= 0.204\times10^{-4}\,\mathrm{m^2\,s^{-1}}$ and $< T^{(\mathrm{b})}_{\mathrm{well}} >= 1.11\times10^{-4}\,\mathrm{m^2\,s^{-1}}$, which is in both cases far from the theoretical harmonic mean value $T_\mathrm{H} = 0.61\times10^{-4}\,\mathrm{m^2\,s^{-1}}$ as being the representative value for the near well behavior.

Inverse estimation results for the realization in Fig. 3a differ for the drawdowns along the four axial directions $\langle h(r,\phi_j)\rangle$ and the radial mean $\langle h(r)\rangle$: the estimated geometric mean ranges between 1.03×10^{-4} and $1.45\times10^{-4}\,\mathrm{m^2\,s^{-1}}$ for the four axial directions, with an average value of $\hat{T}_\mathrm{G}=1.17\times10^{-4}\,\mathrm{m^2\,s^{-1}}$. The estimates for the local transmissivity at the well are between 0.195×10^{-4} and $0.212\times10^{-4}\,\mathrm{m^2\,s^{-1}}$, with an average value of $\hat{T}_\mathrm{well}=0.204\times10^{-4}\,\mathrm{m^2\,s^{-1}}$, which is exactly the sampled local transmissivity $<T_\mathrm{well}^{(a)}>$. The value of $\hat{T}_\mathrm{well}=0.204\times10^{-4}\,\mathrm{m^2\,s^{-1}}$ is equivalent to a local variance of $\hat{\sigma}^2=3.49$. The estimated correlation length ranges between 7.95 and $18.15\,\mathrm{m}$, with an average of $\hat{\ell}=12.77\,\mathrm{m}$. The differences in the estimates for the drawdowns in different direction for the same realization of transmissivity shows that the parameter estimates reflect local heterogeneity in the vicinity of the well rather than the global statistical parameters of the transmissivity field. This was studied and discussed in detail for pumping tests in three dimensional heterogeneous media by Zech et al. (2015).

The realization in Fig. 3b does not allow to infer the parameters of variance and correlation length, due to the similarity of T_well and T_G. Near and far field representative transmissivities are nearly identical, thus the pumping test appears to behave like in a homogeneous medium (Fig. 3b). However, the behavior is not representative but a result of the coincidental choice of the location of the pumping well.

A statistical analysis of the estimation results is presented in Fig. 4 for all 5000 realizations of Ensemble A. Histogram on the best fitting estimates in normalized form are shown, where normalization of results means that they were divided by the input parameters. It can be inferred that the estimate of the geometric mean $\hat{T}_\mathrm{G}$ is in general close to the input value T_G. The estimate of the local transmissivity at the well $\hat{T}_\mathrm{well}$ is very close to the sampled values $<T_\mathrm{well}>$ for nearly all realizations. Thus, the method reproduced very well the local transmissivity at the well. However, the local value T_well of every realization can be far from the theoretical value of T_H, where both realizations in Fig. 3 gave example. The estimates of the correlation length show a very large scatter. Exceptionally large and small value for $\hat{\ell}$ refer to realizations, where it was nearly impossible to infer it due to the similarity of T_well and T_G, as for the realization of Fig. 3b. The large range of estimated correlation lengths also point towards the fact that $\hat{\ell}$ of a single drawdown needs to be interpreted as a local value, which is determined by the transmissivity distribution in the vicinity of the well rather than the distribution of the entire field. However, the median of the normalized estimated correlation lengths is close to one, pointing to the fact that representative values can be inferred by taking the mean from multiple pumping tests.

4 Application Example: Single Aquifer Analysis

Pumping test campaigns in the field often include the performance of multiple pumping tests within one aquifer. Drawdown measurements at multiple test locations can be used to gain representative

parameters of the heterogeneous transmissivity field. The sampled area increases and the effect of local heterogeneity reduces. In the following, it is shown, how mean T_{G}, variance σ^2 and the correlation length ℓ of an individual transmissivity fields can be inferred making use of a sampling strategy in combination with $h_{\mathrm{efw}}^{\mathrm{local}}(r)$.

4.1 Sampling Strategy

The sampling strategy was constructed as pumping test campaign in a virtual aquifer with heterogeneous transmissivity. A series of steady state pumping tests was performed at n different wells. For each test, drawdowns were measured at all n wells and at m additional observation wells. A similar sampling strategy to infer the aquifer statistics from drawdown measurements have been pursued by e.g. Neuman et al. (2004); Copty and Findikakis (2004); Firmani et al. (2006).

The used sampling strategy includes $n = 8$ pumping wells and $m = 4$ observation wells. The specific location of all wells are indicated in Fig. 5. All 8 pumping wells are located within a distance of $18\,\mathrm{m}$. The observation wells are located at larger distances and in all four directions. The well locations were designed to gain numerous drawdown measurements in the vicinity of each pumping well to allow a reliable estimation of T_{well} (or $\sigma^2_{\mathrm{local}}$, respectively) and ℓ. The additional observation wells provide head observations in the far field to gain a representative value for T_{G}. The choice of the well locations does not interfere with the refinement of the numerical grid at the pumping well.

Each of the 8 pumping tests was analyzed with $h_{\mathrm{efw}}^{\mathrm{local}}(r)$ (Sect. 2.4). The best fitting estimates $\hat{T}_{\mathrm{G}}$, $\hat{T}_{\mathrm{well}}$, and $\hat{\ell}$ for all tests were inferred by minimizing the difference between the analytical solution and the 12 measurements. Additionally, parameter estimates were inferred by analyzing the drawdown measurements of all tests jointly.

4.2 Aquifer Analysis

The sampling strategy was applied to fields of all ensembles A-G (Table 1). Results are presented for two fields: D1 out of Ensemble D ($\sigma^2 = 2.25$, $\ell = 20\,\mathrm{m}$) and E1 out of Ensemble E ($\sigma^2 = 4.0$, $\ell = 10\,\mathrm{m}$). Each field was generated according to the theoretical values defined for the particular ensemble and afterwards analyzed geostatistically to determine the sampled values. The fields D1 and E1 are visualized in Fig. 5. The drawdown measurements for all 8 pumping tests at both fields are given in Fig. 6. The inverse estimates as well as theoretical input and sampling values for the statistical parameters are summarized in Table 2.

Analyzing the data from all 8 pumping tests at field D1 jointly yields very close estimates of all parameters $\hat{T}_{\mathrm{G}}$, $\hat{T}_{\mathrm{well}}$ (corresponding to $\hat{\sigma}^2 = 2.255$), and $\hat{\ell}$ to the theoretical and sampled values. The geometric mean estimate is similar for all of the 8 individual pumping tests. In contrast, the values of $\hat{T}_{\mathrm{well}}$ vary within one order of magnitude. This behavior was expected, since $\hat{T}_{\mathrm{well}}$ represents the local transmissivity value at the pumping well. The wide range of estimates is a results of the high variance of the transmissivity field. The estimates of the correlation length $\hat{\ell}$ differ between

the individual tests within a reasonable range of a few meters. The only exception is the estimate for pumping at PW_5. For this specific pumping test is highly uncertain due to the coincidence of the values of $\hat{T}_{\mathrm{well}}$ and $\hat{T}_{\mathrm{G}}$, similar to the realizations in Fig. 3b, as discussed in section 3.3. However, the mean value over the individual tests as well as the estimate from the joint analysis of all measurements gave reliable estimates for the correlation length.

The analysis of the sampling strategy at field E1 yields similar results as for D1. The geometric mean values $\hat{T}_{\mathrm{G}}$ differ little among the 8 individual pumping tests and for the joint analysis. The mean value is double the value as the theoretical one, but close to the sampled geometric mean (Table 2). The local transmissivities $\hat{T}_{\mathrm{well}}$ again vary within one order of magnitude, reflecting the high variance of the field. The mean and jointly estimated values are higher than theoretical one, which is in correspondence to the difference in the geometric mean. The estimates of the correlation length $\hat{\ell}$ deviate in a reasonable range of a few meters, which reflects the impact of the location of the pumping well with regard to the shape of the correlation structure around the well.

Finally, the analysis shows that representative values of the statistical parameters can be determined by performing pumping test at multiple locations of an individual transmissivity field. It was shown, that $h_{\mathrm{efw}}(r)$ is feasible to interpret steady state pumping tests in highly heterogeneous fields.

5 Conclusions

The analytical effective well flow solution $h_{\mathrm{efw}}(r)$ is presented, which can be interpreted as extension of Thiem's equation to heterogeneous media. $h_{\mathrm{efw}}(r)$ depends on the statistical parameters of log-normal distributed transmissivity: geometric mean T_{G}, variance σ^2 and correlation length ℓ. $h_{\mathrm{efw}}(r)$ was derived based on the Radial Coarse Graining transmissivity $T_{\mathrm{RCG}}(r)$ introduced by Schneider and Attinger (2008), which interpolates between the near well and far field representative transmissivities for well flow. Simulation of pumping tests were performed in log-normally distributed transmissivity fields and compared with $h_{\mathrm{efw}}(r)$. Based on the results, the following conclusions can be drawn:

1. $h_{\mathrm{efw}}(r)$ describes the mean drawdown of a pumping test in two dimensional heterogeneous isotropic media effectively. It is not limited to small variance, but is tested to reproduce ensemble means for highly heterogeneous media with variances up to $\sigma^2 = 4$.

2. The analytical character of $h_{\mathrm{efw}}(r)$ allows to perform inverse estimation of the statistical parameters of the transmissivity fields from measured drawdowns. Geometric mean T_{G}, variances σ^2 and correlation length ℓ can be estimated for a wide range of parameters with a high accuracy and certainty from ensemble mean drawdowns.

3. Parameter estimates from individual drawdowns reflect local heterogeneity at the well rather than the global statistical parameters of the transmissivity field.

4. Representative values of geometric mean, variance and correlation length for an individual field of transmissivity can be determined by performing pumping test at multiple locations of that field, estimating the parameters for every test separately and than performing a statistical analysis of the results.

$h_{\mathrm{efw}}(r)$ is a promising tool to interpret steady state pumping tests in order to infer the statistical parameters of the underlying transmissivity field without time- and cost-intensive laboratory investigations. Future steps will include the expansion of the method to interpret transient pumping test data.

The article processing charges for this open-access publication were covered by a Research Centre of the Helmholtz Association.

The effective well flow head $h_{\mathrm{efw}}(r)$ as solution of the well flow equation (2) is derived by solving the integral (Eq. 3) with the analytical expression of $T_{\mathrm{RCG}}(r)$ from Eq. (4).

$$h(r_2) - h(r_1) = \frac{C_1}{T_{\mathrm{G}}} \int_{r_1}^{r_2} \frac{1}{r} \exp\left(\frac{\sigma^2}{2} \frac{1}{(1+\zeta^2 r^2/\ell^2)} \right) \mathrm{d}r \,. \tag{A1}$$

The integral is evaluated analytically by making use of the exponential integral function

$$\Gamma(x) - \Gamma(X) = \int_X^x \frac{\exp(z)}{z} \,\mathrm{d}z = \ln\frac{x}{X} + \sum_{k=1}^{\infty} \frac{x^k - X^k}{k!k} \,. \tag{A2}$$

The argument in the exponent in Eq. (A1) is substituted by $z(r) = \frac{\sigma^2}{2} \frac{1}{(1+\zeta^2 r^2/\ell^2)}$ with integrator $\mathrm{d}r = -\frac{\ell\sigma^2}{4\zeta z^2} \left(\frac{\sigma^2}{2z} - 1 \right)^{-\frac{1}{2}} \mathrm{d}z$, furthermore partial fraction decomposition is used, resulting in

$$\begin{aligned} h(r_2) - h(r_1) &= \frac{C_1}{T_{\mathrm{G}}} \frac{\sigma^2}{4} \int_{z(r_1)}^{z(r_2)} \frac{\exp(z)}{z(z-\frac{\sigma^2}{2})} \,\mathrm{d}z \\ &= \frac{C_1}{2T_{\mathrm{G}}} \int_{z(r_1)-\frac{\sigma^2}{2}}^{z(r_2)-\frac{\sigma^2}{2}} \frac{\exp\left(z+\frac{\sigma^2}{2}\right)}{z} \,\mathrm{d}z - \frac{C_1}{2T_{\mathrm{G}}} \int_{z(r_1)}^{z(r_2)} \frac{\exp(z)}{z} \,\mathrm{d}z \\ &= \frac{C_1}{2T_{\mathrm{G}}} \mathrm{e}^{\frac{\sigma^2}{2}} \left(\Gamma\left(z(r_2) - \frac{\sigma^2}{2} \right) - \Gamma\left(z(r_1) - \frac{\sigma^2}{2} \right) \right) \\ &\quad - \frac{C_1}{2T_{\mathrm{G}}} \left(\Gamma(z(r_2)) - \Gamma(z(r_1)) \right) . \end{aligned} \tag{A3}$$

The final solution for the effective well flow head as given in Eq. (6) results by re-substituting the abbreviation $z(r) = \frac{\sigma^2}{2} \frac{1}{(1+\zeta^2 r^2/\ell^2)}$ with $r_2 = r$ and $r_1 = R$ and inserting $C_1 = -\frac{Q_{\mathrm{w}}}{2\pi}$ as derived from the constant flux boundary condition (Sect. 2.1).

An approximate formulation of Eq. (A3) can be derived by using the definition of the exponential integral function as infinite sum, given in Eq. (A2) in combination with the relationship $z(r) - \frac{\sigma^2}{2} =$

$\frac{\sigma^2}{2}\frac{-\zeta^2 r^2/\ell^2}{1-\zeta^2 r^2/\ell^2} = z(r)\left(-\frac{\zeta^2 r^2}{\ell^2}\right)$:

$$
\begin{aligned}
h(r_2) - h(r_1) = {} & \frac{C_1}{2T_\mathrm{G}} \mathrm{e}^{\frac{\sigma^2}{2}} \left(\ln \frac{z(r_2) - \frac{\sigma^2}{2}}{z(r_1) - \frac{\sigma^2}{2}} + \sum_{k=1}^{\infty} \frac{\left(z(r_2) - \frac{\sigma^2}{2}\right)^k - \left(z(r_1) - \frac{\sigma^2}{2}\right)^k}{k!k} \right) \\
& - \frac{C_1}{2T_\mathrm{G}} \left(\ln \frac{z(r_2)}{z(r_1)} + \sum_{k=1}^{\infty} \frac{z(r_2)^k - z(r_1)^k}{k!k} \right) \\
= {} & \frac{C_1}{T_\mathrm{G}} \mathrm{e}^{\frac{\sigma^2}{2}} \ln \frac{r_2}{r_1} + \frac{C_1}{2T_\mathrm{G}} \left(\mathrm{e}^{\frac{\sigma^2}{2}} - 1 \right) \ln \frac{z(r_2)}{z(r_1)} \\
& + \frac{C_1}{2T_\mathrm{G}} \sum_{k=1}^{\infty} \frac{z(r_2)^k \left(\mathrm{e}^{\frac{\sigma^2}{2}} (-\zeta^2 r_2^2/\ell^2)^k - 1 \right) - z(r_1)^k \left(\mathrm{e}^{\frac{\sigma^2}{2}} (-\zeta^2 r_1^2/\ell^2)^k - 1 \right)}{k!k} \\
\approx {} & \frac{C_1}{T_\mathrm{G}} \mathrm{e}^{\frac{\sigma^2}{2}} \ln \frac{r_2}{r_1} + \frac{C_1}{2T_\mathrm{G}} \left(\mathrm{e}^{\frac{\sigma^2}{2}} - 1 \right) \ln \frac{z(r_2)}{z(r_1)} + \frac{C_1}{2T_\mathrm{G}} \left(\mathrm{e}^{\frac{\sigma^2}{2}} - 1 \right) (z(r_2) - z(r_1)) .
\end{aligned}
\tag{A4}
$$

The final approximate solution as given in Eq. (7) results by re-substituting $z(r)$ with $r_2 = r$ and $r_1 = R$ and inserting $C_1 = -\frac{Q_\mathrm{w}}{2\pi}$.

References

Attinger, S.: Generalized coarse graining procedures for flow in porous media, Comput. Geosci., 7, 253–273, doi:10.1023/B:COMG.0000005243.73381.e3, 2003.

Copty, N. K., and A. N. Findikakis, Stochastic analysis of pumping test drawdown data in heterogeneous geologic formations, *J. Hydraul. Res.*, *42, EXTRA ISSUE*, 59–67, doi:10.1080/00221680409500048, 2004.

Dagan, G., *Flow and Transport on Porous Formations*, Springer, New York, 1989.

Dagan, G. and Lessoff, S. C.: Transmissivity upscaling in numerical aquifer models of steady well flow: unconditional statistics, Water Resour. Res., 43, W05431, doi:10.1029/2006WR005235, 2007.

Desbarats, A.: Spatial averaging of transmissivity in heterogeneous fields with flow toward a well, Water Resour. Res., 28, 757–767, doi:10.1029/91WR03099, 1992.

Firmani, G., A. Fiori, and A. Bellin, Three-dimensional numerical analysis of steady state pumping tests in heterogeneous confined aquifers, *Water Resour. Res.*, *42*, W03422, doi:10.1029/2005WR004382, 2006.

Gelhar, L.: Stochastic Subsurface Hydrology, Prentice Hall, Englewood Cliffs, New York, 1993.

Heße, F., Prykhodko, V., Schlüter, S., and Attinger, S.: Generating random fields with a truncated power-law variogram: a comparison of several numerical methods, Environ. Modell. Softw., 55, 32–48, doi:10.1016/j.envsoft.2014.01.013, 2014.

Indelman, P., Fiori, A., and Dagan, G.: Steady flow toward wells in heterogeneous formations: mean head and equivalent conductivity, Water Resour. Res., 32, 1975–1984, doi:10.1029/96WR00990, 1996.

Kolditz, O., Görke, U., Shao, H., and Wang, W. (Eds.): Thermo-Hydro-Mechanical-Chemical Processes in Porous Media, Springer Verlag, Berlin Heidelberg, 2012b.

Matheron, G.: Elements Pour Une Theorie des Milieux Poreux, Maisson et Cie, Paris, 1967.

Neuman, S. P., A. Guadagnini, and M. Riva, Type-curve estimation of statistical heterogeneity, *Water Resour. Res.*, *40*, W04201, doi:10.1029/2003WR002405, 2004.

Neuman, S. P., Blattstein, A., Riva, M., Tartakovsky, D., Guadagnini, A., and Ptak, T.: Type curve interpretation of late-time pumping test data in randomly heterogeneous aquifers, Water Resour. Res., 43, W10421, doi:10.1029/2007WR005871, 2007.

Sánchez-Vila, X., Axness, C. L., and Carrera, J.: Upscaling transmissivity under radially convergent flow in heterogeneous media, Water Resour. Res., 35, 613–621, doi:10.1029/1998WR900056, 1999.

Sánchez-Vila, X., Guadagnini, A., and Carrera, J.: Representative hydraulic conductivities in saturated groundwater flow, Rev. Geophys., 44, RG3002, doi:10.1029/2005RG000169, 2006.

Schneider, C. L. and Attinger, S.: Beyond Thiem – a new method for interpreting large scale pumping tests in heterogeneous aquifers, Water Resour. Res., 44, W04427, doi:10.1029/2007WR005898, 2008.

Thiem, G.: Hydrologische Methoden, J. M. Gebhardt, Leipzig, 1906.

Zech, A., Schneider, C. L., and Attinger, S.: The extended Thiem's solution – including the impact of heterogeneity, Water Resour. Res., 48, W10535, doi:10.1029/2012WR011852, 2012.

Zech, A., Arnold, S., Schneider, C., and Attinger, S.: Estimating Parameters of Aquifer Heterogeneity Using Pumping Tests – Implications for Field Applications, Adv. Water Resour., 83, 137–147, doi:10.1016/j.advwatres.2015.05.021, 2015.

Table 1. Ensemble input parameters T_G, σ^2 and ℓ and best fitting inverse estimation results $\hat{T}_\mathrm{G}$, $\hat{\sigma}^2$ and $\hat{\ell}$ with $95\,\%$ confidence intervals (in brackets) for ensemble mean $\overline{\langle h(r)\rangle}$ for all generated ensembles.

	T_G	$\hat{T}_\mathrm{G}$ $[10^{-4}\,\mathrm{m^2\,s^{-1}}]$	σ^2	$\hat{\sigma}^2$ $[-]$	ℓ	$\hat{\ell}$ [m]
A	1.0	1.03 ($\pm$0.0011)	1.0	1.04 ($\pm$0.0022)	10	9.80 ($\pm$0.086)
B	1.0	1.08 ($\pm$0.0013)	1.0	1.19 ($\pm$0.0022)	20	21.6 ($\pm$0.127)
C	1.0	1.08 ($\pm$0.0021)	2.25	2.49 ($\pm$0.0038)	10	10.1 ($\pm$0.050)
D	1.0	1.19 ($\pm$0.0024)	2.25	2.67 ($\pm$0.0039)	20	22.2 ($\pm$0.077)
E	1.0	1.16 ($\pm$0.0046)	4.0	4.34 ($\pm$0.0078)	10	11.0 ($\pm$0.042)
F	1.0	1.31 ($\pm$0.0088)	4.0	4.27 ($\pm$0.0131)	20	22.2 ($\pm$0.120)
G	1.5	1.55 ($\pm$0.0012)	1.0	1.03 ($\pm$0.0016)	10	10.1 ($\pm$0.066)

Table 2. Parameter estimates of geometric mean transmissivity $\hat{T}_\mathrm{G}$ $[10^{-4}\,\mathrm{m^2/s}]$, local transmissivity at the well $\hat{T}_\mathrm{well}$ $[10^{-4}\,\mathrm{m^2/s}]$ and correlation length $\hat{\ell}$ [m] for the 8 pumping tests at fields D1 (from Ensemble D, $\sigma^2 = 2.25$) and E1 (from Ensemble E, $\sigma^2 = 4.0$). Additionally, the theoretical and the sampled values ($T_\mathrm{well} \equiv T_\mathrm{H}$) are given.

	D1			E1		
	$\hat{T}_\mathrm{G}$	$\hat{T}_\mathrm{well}$	$\hat{\ell}$	$\hat{T}_\mathrm{G}$	$\hat{T}_\mathrm{well}$	$\hat{\ell}$
PW_0	1.025	0.434	29.51	1.945	0.313	9.56
PW_1	1.023	0.362	27.23	2.202	0.445	11.55
PW_2	1.076	0.220	23.68	2.093	0.437	10.03
PW_3	0.898	1.057	9.51	2.052	0.520	15.34
PW_4	1.001	0.147	20.53	2.174	1.847	12.30
PW_5	0.889	1.071	5.33	1.980	1.117	5.43
PW_6	1.038	0.177	20.39	1.840	0.148	8.78
PW_7	0.901	1.700	16.48	1.969	0.476	17.04
Mean of 8	0.981	0.646	19.08	2.032	0.663	9.90
Jointly	1.013	0.328	22.38	2.010	0.409	9.97
Theory	1.0	0.325	20.0	1.0	0.135	10.0
Sampled	0.985	0.333	23.43	1.999	0.491	12.66

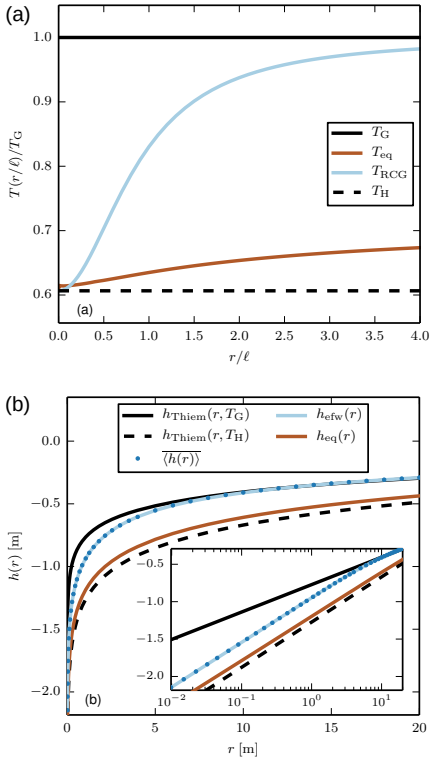

Figure 1. Comparison of equivalent and Radial Coarse Graining approach: **(a)** radially depending transmissivities interpolating between harmonic mean T_H and geometric mean T_G: $T_{RCG}(r)$ from Eq. (4) and $T_{eq}(r)$ calculated based on Thiem's formula Eq. (1) with $h(r) = \overline{\langle h(r)\rangle}$, which is the ensemble mean for Ensemble A (Table 1), **(b)** hydraulic head drawdowns after pumping with: $h_{efw}(r)$ from Eq. (6) as solution of the well flow equation using $T_{RCG}(r)$, $h_{eq}(r)$ as solution of the well flow equation using $T_{eq}(r)$, Thiem's solution with homogeneous substitute values T_G and T_H as well as mean ensemble drawdown $\overline{\langle h(r)\rangle}$.

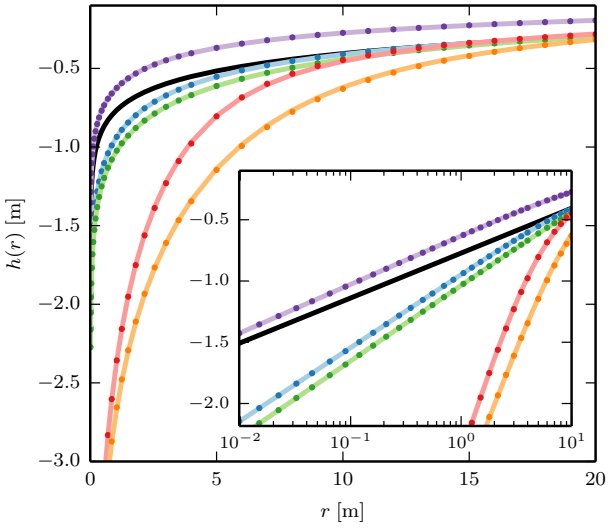

Figure 2. Simulated ensemble means $\overline{\langle h(r) \rangle}$ (dots) and $h_{\text{efw}}(r)$ with best fitting estimates (lines) for multiple Ensembles: A (blue), B (green), E (red), F (orange), G (purple). Parameter values are listed in Table 1. Black line shows $h_{\text{Thiem}}(r)$ with $T_{\text{G}} = 10^{-4}\,\text{m}^2\,\text{s}^{-1}$.

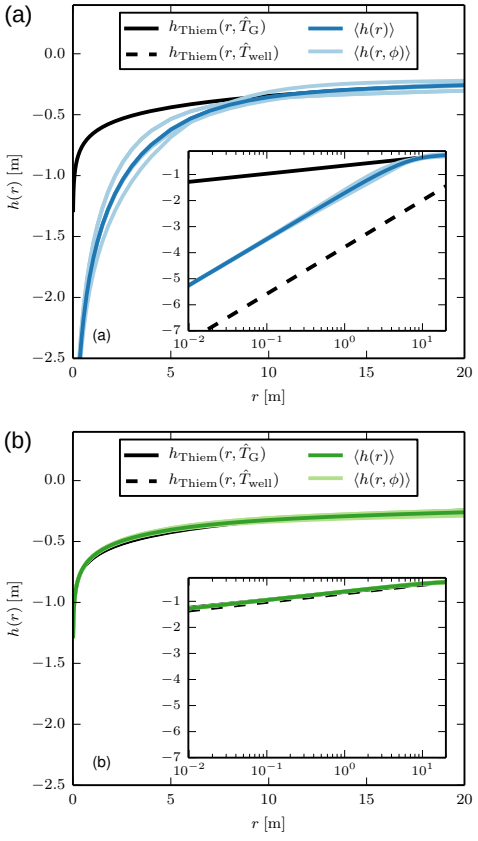

Figure 3. Drawdowns simulated for two individual transmissivity field realizations of Ensemble A ($T_{\mathrm{G}} = 10^{-4}\,\mathrm{m^2\,s^{-1}}$, $\sigma^2 = 1$, $\ell = 10\,\mathrm{m}$): **(a)** realization with $T_{\mathrm{well}} = 0.204 \times 10^{-4}\,\mathrm{m^2\,s^{-1}}$ and **(b)** realization with $T_{\mathrm{well}} = 1.11 \times 10^{-4}\,\mathrm{m^2\,s^{-1}}$. $\langle h(r) \rangle$ (dark color) is the radial mean, $\langle h(r, \phi) \rangle$ (light color) denotes the drawdowns along the four axes ($\phi = 0°, 90°, 180°, 270°$), as well as in black Thiem's solution for homogeneous substitute values.

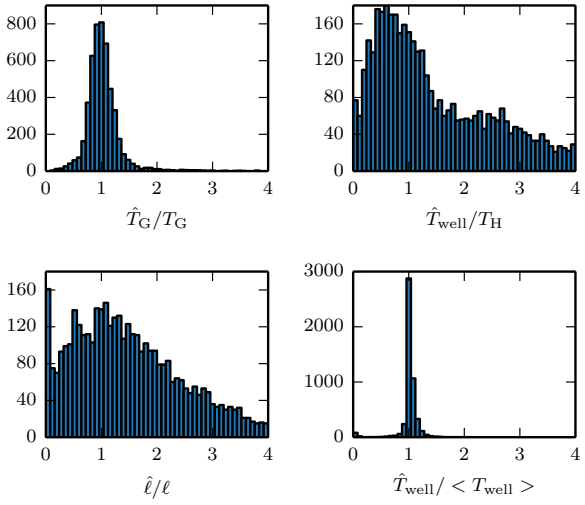

Figure 4. Histogram on the best fitting estimates ($\hat{T}_{\rm G}$, $\hat{T}_{\rm well}$, $\hat{\ell}$) versus the theoretical input values ($T_{\rm G}$, $T_{\rm H}$,ℓ) and the sampled transmissivity at the pumping well ($< T_{\rm well} >$) for the $N = 5000$ realizations of Ensemble A.

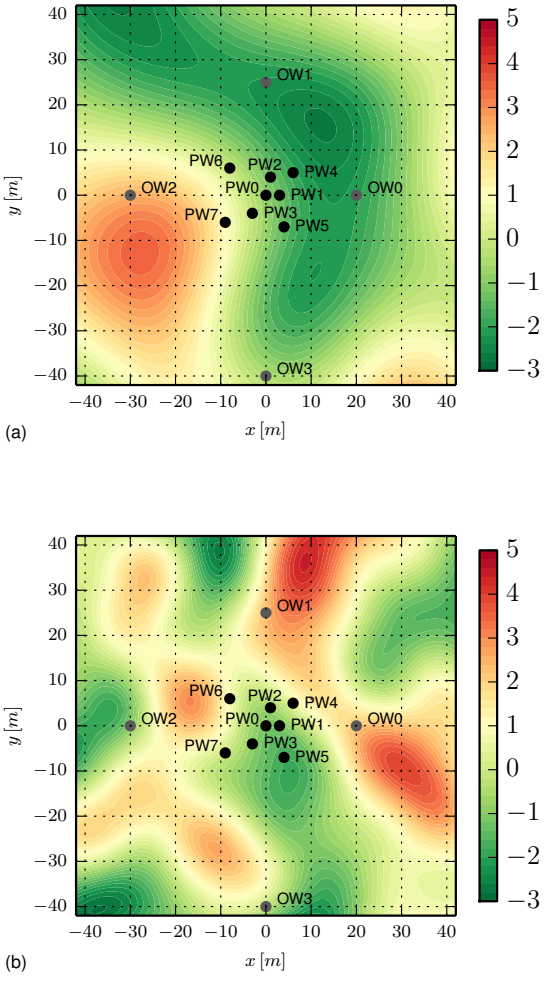

Figure 5. Spatial distribution of log-transmissivity for fields (a) D1 and (b) E1 and locations of the eight pumping wells ($PW_0,\ldots,PW_7$ in black) and the four observation wells ($OW_0,\ldots,OW_3$ in gray).

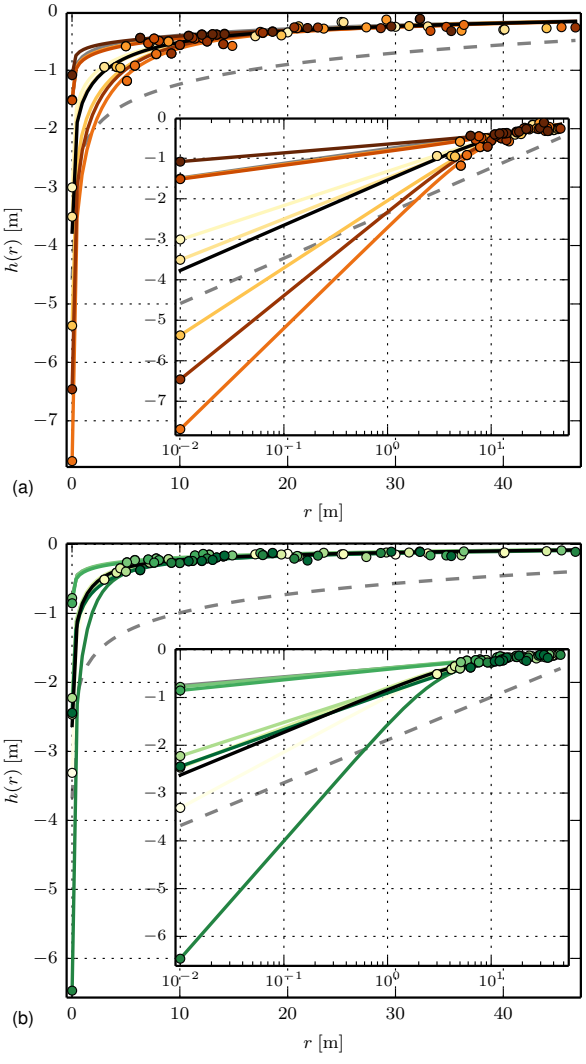

Figure 6. Simulated drawdown measurements (dots) and fitted effective well flow solution $h_{\mathrm{efw}}(r)$ (lines) for eight pumping tests within the heterogeneous transmissivity fields (a) D1 and (b) E1. Colours indicate the results for the individual pumping tests at $\mathrm{PW}_0, \ldots, \mathrm{PW}_7$ (from light to dark). The black line denotes the effective well flow solution $h_{\mathrm{efw}}(r)$ fitted to all measurements jointly. Gray lines denote Thiem's solution for $\hat{T}_{\mathrm{G}}$ (solid) and for $\hat{T}_{\mathrm{well}}$ (dashed). Statistical parameters are given in Table 2.